RSC Advances

PAPER

View Article Online
View Journal | View Issue

Cite this: *RSC Adv.*, 2022, **12**, 22236

Construction of carbon-based flame retardant composite with reinforced and toughened property and its application in polylactic acid

Yunchao Xiao, [ab] Yaru Yang,*[a] Qiulan Luo,[c] Bolin Tang, [ab] Jipeng Guan[a] and Qiang Tian[d]

To simultaneously improve the flame retardancy, strength and toughness of polylactic acid (PLA) fibers, a composite flame retardant CNTs-H-C was prepared with carbon nanotubes (CNTs) as the core, hexachlorocyclotriphosphazene as linker, and chitosan grafted on the surface. The prepared CNTs-H-C was introduced into a PLA matrix to obtain CNTs-H-C/PLA composites and fibers *via* a melt-blending method. The morphology, structure, flame retardant properties and mechanical properties were thoroughly characterized, and the flame retardant mechanism was studied. Results showed that the prepared CNTs-H-C displayed a nanotube-like morphology with good compatibility and dispersion in the PLA matrix. After blending with PLA, CNTs-H-C/PLA composites exhibited outstanding flame retardancy with limiting oxygen index (LOI) increasing from 20.0% to 27.3%, UL94 rating reaching V-0. More importantly, the introduction of CNTs-H-C did not affect the spinnability of PLA. Compared with pure PLA fibers, the LOI of CNTs-H-C/PLA fibers with a CNTs-H-C content of 1.0 wt% increased by 32.5%, and meanwhile the breaking strength and elongation increased by 28.2% and 30.4%, respectively. Mechanism study revealed that CNTs-H-C/PLA possessed a typical condensed phase flame retardancy mechanism. In short, we have developed a CNT-based composite flame retardant with reinforced and toughened properties for the PLA matrix. The prepared CNTs-H-C showed great potential in polymer flame retardancy and mechanical enhancement.

Received 4th July 2022
Accepted 29th July 2022

DOI: 10.1039/d2ra04130h

rsc.li/rsc-advances

Introduction

Polylactic acid (PLA) has attracted much attention in the past decades, due to its excellent processing performance and sustainable starch-derived source.[1–3] As a thoroughly biodegradable polymer, PLA can be decomposed into carbon dioxide and water by microorganisms in soil or seawater.[4,5] Therefore, PLA is considered as an ideal material to replace petroleum-based polymers. At present, PLA has been applied in the fields of food packaging, medical and health care, and 3D printing. Especially, when processed into fibers and fabrics, PLA exhibits outstanding hand feeling, drape and UV resistance, which is very suitable for fashion, casual wear and sanitary products, and has extensive prospects.[6,7] However, PLA is rarely seen in the fields of transportation, aerospace, and home textiles, mainly due to the defects of flammability, low strength, and poor toughness of PLA.[8–12] For this reason, the flame retardant modification and mechanical improvement have always been the focus for PLA.

To date, the common method to improve the flame retardancy of PLA is to introduce halogen-containing, phosphorus-containing or intumescent flame retardants.[13] However, the use of halogen-based flame retardants is limited due to the toxicity of their combustion products,[14] while phosphorus-based flame retardants and intumescent flame retardants often have problems such as large additions, damage to the mechanical properties of PLA, and difficulty in spinning.[15,16] How to simultaneously improve the flame retardancy, strength and toughness of PLA is still a tough challenge.

In recent decades, with the vigorous development of carbon nanomaterials, carbon nanotubes (CNTs) have been widely used as reinforcement and toughening materials for polymers.[17] For instance, Liu *et al.*[18] added block copolymer-modified multi-walled carbon nanotubes (bc@fMWNTs) to epoxy resin (EP) to prepare nanocomposites and showed that only 0.05 wt% bc@fMWNTs could achieve 15% increase in tensile strength of EP. Moreover, numerous studies have shown that CNTs can be used as flame retardant additives for polymers, and adding a very small amount of CNTs can effectively reduce the heat release rate of the polymers.[19,20] However, the flame retardant effect of pure CNTs is limited, and it is often necessary to

[a]*College of Materials and Textile Engineering, Jiaxing University, Jiaxing 314001, Zhejiang, China*
[b]*Nanotechnology Research Institute, Jiaxing University, Jiaxing 314001, Zhejiang, China*
[c]*College of Fashion Design, Jiaxing Nanhu University, Jiaxing 314001, Zhejiang, China*
[d]*Zibo Dayang Flame Retardant Products Co., Ltd., Zibo 255300, Shandong, China*

improve the flame retardant efficiency of CNTs by surface modification or compounding with other flame retardants.[21] For example, Zhang *et al.*[22] prepared 3-glycidoxypropyltrimethoxysilane (GPTES) functionalized multi-walled carbon nanotubes (f-CNTs), which were mixed with graphite sheets (GSs) and then added into EP to prepare composites. The research shows that when the mass fraction of f-CNTs/GSs is 3.9 wt%, the LOI of EP is increased to 27.4%, and the tensile strength and notched impact strength are increased by 33.5% and 44.8%, respectively. And the electrical conductivity of the composite material increases with the increase of carbon nanotube content. In addition, our previous studies have demonstrated that CNTs have a significant effect on droplet suppression of polymers.[23] More importantly, CNTs did not affect the spinnability of fibers. Therefore, selecting CNTs to synthesize composite flame retardants is expected to achieve both flame retardancy and toughening effects in PLA.

Chitosan (CS) is a natural, readily available alkaline polysaccharide, which is non-toxic and harmless, and has excellent biocompatibility, microbial degradability and processability. With plenty of hydroxyl groups and amino groups, as well as carbon element in molecular skeleton, CS can be decomposed to generate a large amount of incombustible gases such as CO_2, N_2 and NH_3. For this reason, CS is able to act as a green flame retardant. However, the flame retardant effect of pure CS is not sufficient, so it is always combined with phosphorus-containing components to form composite flame retardants.[24–26]

Hexachlorocyclotriphosphazene (HCCP) is a commonly used intermediate for phosphorus-based flame retardants. Its molecular structure contains six active chlorine atoms, which are easily replaced by various nucleophiles under certain conditions. Therefore, a series of new composite flame retardants can be prepared by flexibly utilizing the substitution reaction of HCCP.[27,28]

Aiming to simultaneously improve the flame retardancy, strength and toughness without affecting the spinnability of PLA, a CNT-based flame retardant was synthesized and introduced into PLA. By using CNTs as the core, HCCP as the bridge, and CS as the surface grafting agent, a non-halogenated, nanosized, synergistic, and low-added carbon-based composite flame retardant CNTs-H-C was prepared, as shown in Fig. 1. The CNTs-H-C/PLA composites and fibers were obtained by melt blending and melt spinning. In the present study, the morphology, structure, flame retardant properties and mechanical properties were thoroughly characterized, and the flame retardant mechanism of CNTs-H-C in PLA was also investigated.

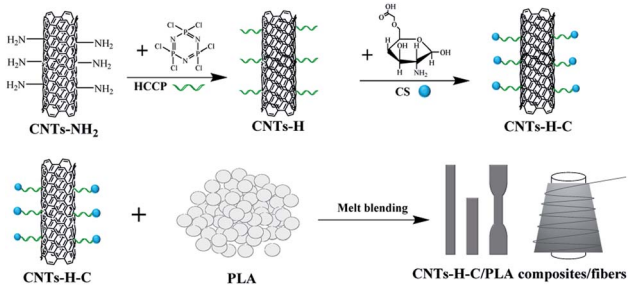

Fig. 1 Schematic illustration of the construction of CNTs-H-C and the preparation of CNTs-H-C/PLA composites and fibers.

Experimental

Materials

Polylactic acid (PLA, $M_w = 100\,000$) was purchased from Anhui Fengyuan Futailai Polylactic Acid Co., Ltd.; carboxymethyl chitosan (CS, deacetylation degree ≥95%) was acquired from Shanghai Aladdin Biochemical Technology Co., Ltd; carboxylated multi-wall carbon nanotubes (CNTs, 99.9%) were received from Shenzhen Yuechuang Technology Co., Ltd.; hexachlorocyclotriphosphazene (HCCP) was supplied by Zibo Lanyin Chemical Co., Ltd.; triethylamine (TEA, AR) was obtained from Tianjin Guangfu Institute of Fine Chemicals; tetrahydrofuran (THF, AR) was provided by Shanghai Lianshi Chemical Co., Ltd.; all chemical reagents were used as received.

Preparation of CNTs-H-C flame retardant

Firstly, aminated carbon nanotubes (CNTs-NH_2) were prepared according to the literature.[29] In brief, CNTs (2 g) were dispersed in 50 mL of DMF, followed by the addition of 4 g polyethylene polyamine, and reacted for 24 h under nitrogen atmosphere. After washing, filtering, and drying, the CNTs-NH_2 were prepared. The prepared CNTs-NH_2 were dispersed in 75 mL of THF, and ultrasonically treated for 10 min. Then 0.66 g HCCP and 0.3 mL TEA were added into the dispersed CNTs-NH_2 solution, and stirred for 1.5 h at 30 °C. After reaction, the mixture was filtered, rinsed and vacuum-dried to harvest HCCP modified CNTs (CNTs-H). Afterwards, 2 g CNTs-H were redispersed in 75 mL of THF, followed by the addition of 2 wt% carboxymethyl chitosan aqueous solution (50 mL) and 0.3 mL of triethylamine. After reacted for 6 h at 30 °C, the mixture was centrifuged and washed with anhydrous ethanol and deionized water, and subsequently freeze-dried to obtain the flame retardant of CNTs-H-C.

Preparation of CNTs-H-C/PLA composites and fibers

The pre-dried PLA slices and CNTs-H-C flame retardant were mixed uniformly and fed into the torque rheometer to obtain CNTs-H-C/PLA composite masterbatch. And the obtained CNTs-H-C/PLA composite masterbatch was processed into CNTs-H-C/PLA standard testing-samples by using injection molding machine and flat vulcanizer. For better description, we defined CNTs-H-C/PLA composites with CNTs-H-C content of 1 wt%, 3 wt%, 5 wt% as CNTs-H-C/PLA-1, CNTs-H-C/PLA-3, CNTs-H-C/PLA-5, respectively. Meanwhile, CNTs/PLA composites were also prepared for comparison. In addition, CNTs-H-C/PLA fibers were prepared using a LHFJ030 melt spinning machine, and the spinning parameters were set as: temperature of 190 °C, draft ratio of 3.0.

Characterization

JSM-6510LA scanning electron microscope (SEM, JEOL, Japan) was adopted to investigate the morphology of CNTs-H-C, CNTs-

H-C/PLA fibers and char residues, as well as the tensile fracture of CNTs-H-C/PLA composites. Fourier transform infrared spectrometer (FTIR, PerkinElmer, USA) was used to analyze the chemical structures of the CNTs-H-C flame retardant. The thermal stability and thermal decomposition behavior of CNTs-H-C flame retardants and CNTs-H-C/PLA composites were determined by a TGA 4000 thermogravimetric analyzer (PerkinElmer, USA). The limiting oxygen index (LOI) of pure PLA and CNTs-H-C/PLA composites and fibers was tested by TM606 digital oxygen index tester (Chengde Juyuan Testing Equipment Manufacturing Co., Ltd., China) according to ISO4589-2. The vertical combustion properties of pure PLA and CNTs-H-C/PLA composites were tested using a CZF-5 horizontal and vertical combustion apparatus (Changzhou Dedu Precision Instrument Co., Ltd., China) according to ANSI/UL94-2013. C-1087 cone calorimeter (Suzhou Zhengbiao Combustion Testing Technology Co., Ltd., China) was employed to determine the combustion parameters such as heat release rate (HRR) of pure PLA and CNTs-H-C/PLA composites according to ISO5660-1:2002. The breaking strength and elongation of pure PLA and CNTs-H-C/PLA fibers were measured by a YG061FQ electronic strength tester (Laizhou Yuanmao Instrument Co., Ltd., China) according to ISO2062. The thermal stability and chemical structure of the char residues formed by the combustion of pure PLA and CNTs-H-C/PLA composites in the cone calorimeter was also analyzed using PerkinElmer TGA 4000 thermogravimetric analyzer and FTIR.

Results and discussion

Morphology, structure and thermal stability of CNTs-H-C

To investigate morphology, structure and thermal stability of the prepared CNTs-H-C, SEM, FTIR and TGA was conducted. As can be seen in Fig. 2a, pristine CNTs display smooth surface morphology with a mean tube diameter about 18.7 nm. Compared with CNTs, the surface roughness of CNTs-H-C is significantly increased and the diameter of CNTs-H-C increases to 23.5 nm. It is obvious that a layer of raised particles is attached to the surface of CNTs after modification by HCCP and CS (Fig. 2b). Moreover, SEM equipped with energy dispersive spectroscopy (EDS) was conducted to confirm all the chlorine in HCCP have been substituted in the synthesis process of CNTs-H-C. As shown in Fig. 2c, no chlorine element was detected in CNTs-H-C, visually demonstrating that there is no residual chlorine in CNTs-H-C.

FTIR was employed to confirm the successful synthesis of CNTs-H-C. It can be seen from Fig. 2d that original CNTs display the following characteristic peaks: the characteristic peak of –OH at 3440 cm^{-1} and 1645 cm^{-1}; C–H stretching vibration peaks at 2922 cm^{-1}, 2880 cm^{-1} and 1380 cm^{-1}, characteristic peaks of C=O at 1645 cm^{-1}, C–H stretching vibration peak at 1380 cm^{-1}. In contrast, new characteristic peaks derived from HCCP and CS[30] appear in the infrared spectrum of CNTs-H-C, including: characteristic peaks of P=N at 1366 cm^{-1} and 1210 cm^{-1}, characteristic peaks of P–N at 874 cm^{-1}, characteristic peaks of amide at 1654 cm^{-1} and 1559 cm^{-1}. These indicate that CNTs-H-C was successfully synthesized.

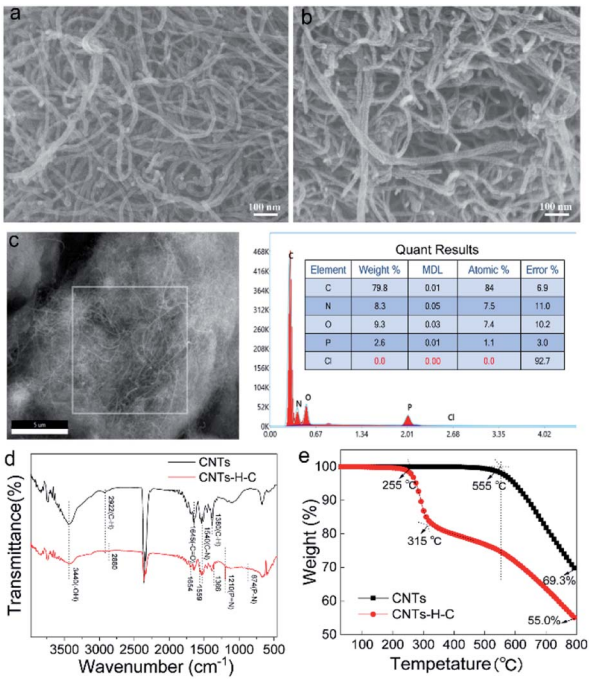

Fig. 2 SEM images ((a) CNTs, (b) CNTs-H-C), EDS detection results of CNTs-H-C (c); infrared spectra (d) and TG curves (e) of CNTs and CNTs-H-C.

Fig. 2e shows the TG curves of CNTs and CNTs-H-C. As can be seen, pristine CNTs exhibit one weight-loss stage from 555 °C in nitrogen atmosphere, corresponding to the decomposition of amorphous carbon of CNTs. Residual mass of CNTs at 800 °C is 69.3%. While CNTs-H-C display two weight-loss stages: the first stage of weight loss occurs from 255 °C to 315 °C, corresponding to the decomposition of HCCP and CS grafted on the surface of CNTs; the second stage of weight loss occurs after 315 °C, attributed to the partial decomposition of HCCP and CS as well as the thermal decomposition of CNTs. The residual mass of CNTs-H-C at 800 °C is 55.0%, and thus the grafted content of HCCP and CS in CNTs-H-C can be calculated as 20.6%.

Flame retardant properties of CNTs-H-C/PLA composites

LOI and UL 94 vertical burning test were performed to study the flame-retardant properties of CNTs-H-C/PLA composites. As shown in Table 1, the LOI value of pure PLA is only 20.0%, which is easily combustible in air. When ignited, the pure PLA burns violently until it burns out, and cannot reach any flame retardant grade (NR). The addition of pristine CNTs significantly improved the anti-dripping property of PLA, but still failed to achieve any flame retardant grade in the UL94 vertical burning test. In contrast, CNTs-H-C/PLA composites exhibit outstanding flame retardancy, with LOI of 25.3–27.3%, and flame retardant grade reaching V-0. And we noted that, the after-flame time (t_1 and t_2) of CNTs-H-C/PLA was significantly shortened and could be rapidly self-extinguished in the UL 94 test, which visually demonstrated that the introduction of CNTs-H-C greatly enhanced the flame retardancy of PLA.[31]

Table 1 LOI and UL 94 vertical burning test results of PLA and CNTs-H-C/PLA[a]

Samples	LOI (%)	UL-94 vertical burning test			
		t_1 (s)	t_2 (s)	Dripping/igniting cotton	Rating
PLA	20.0	>30	>30	Yes/yes	NR
CNTs/PLA-1	21.9	>30	>30	No/no	NR
CNTs/PLA-3	23.0	>30	>30	No/no	NR
CNTs/PLA-5	23.5	>30	>30	No/no	NR
CNTs-H-C/PLA-1	25.3	7.1	5.2	No/no	V-0
CNTs-H-C/PLA-3	27.0	6.3	4.7	No/no	V-0
CNTs-H-C/PLA-5	27.3	5.5	4.3	No/no	V-0

[a] Note: t_1, t_2 represent the combustion time after the first, the second application of the flame. NR-no rating.

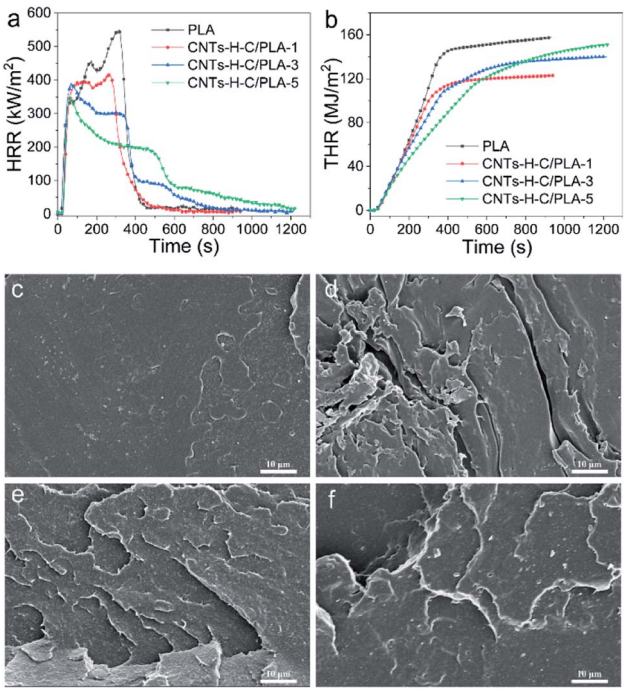

Fig. 3 Heat release rate (a) and total heat release (b) of PLA and CNTs-H-C/PLA; SEM images of the tensile sections of PLA (c) and CNTs-H-C/PLA-1 (d), CNTs-H-C/PLA-3 (e), CNTs-H-C/PLA-5 (f).

Cone calorimeter test

To further evaluate the flame retardant properties of CNTs-H-C, cone calorimeter tests were conducted on PLA and CNTs-H-C/PLA. Heat release rate (HRR) is the main basis for assessing the fire hazard of materials.[32] In Fig. 3a and Table 2, the HRR of pure PLA sharply increases after ignition, and reaches a peak value (pk-HRR) of 552.6 kW m^{-2} at 314 s after ignition. Compared with PLA, the HRR of CNTs-H-C/PLA is significantly reduced, and the pk-HRR of CNTs-H-C/PLA-5 is reduced to 350.8 kW m^{-2}, which is 36.5% lower than that of pure PLA, indicating that the addition of CNTs-H-C can significantly decrease the fire hazard of PLA. With the increase of CNTs-H-C content, the pk-HRR of CNTs-H-C/PLA composites decreases gradually, which is consistent with the LOI test results, suggesting that the flame retardancy of CNTs-H-C/PLA increases with the increase of CNTs-H-C content. It is worth noting that although the HRR curves of PLA and CNTs-H-C/PLA both show two apparent peaks, the heights of the two peaks are significantly different. The HRR of PLA shows a low peak followed by a high peak, which indicates that the heat release of PLA was not suppressed during the combustion process. In contrast, the two peaks of CNTs-H-C/PLA are high first and then low. And the time interval between the two peaks of CNTs-H-C/PLA has been prolonged, so that the HRR curve of CNTs-H-C/PLA tends to be flat, which indicates that the introduction of CNTs-H-C has a significant inhibitory effect on the thermal release of PLA.[33]

Fig. 3b shows the total heat release (THR) during the combustion of PLA and CNTs-H-C/PLA composites. It can be seen that the THR of CNTs-H-C/PLA is lower than that of pure PLA, and the slope of the THR curves of CNTs-H-C/PLA is also smaller than that of pure PLA, which means that the heat release decreases with the introduction of CNTs-H-C. This result is consistent with the HRR analysis that the flame retardant of CNTs-H-C exhibits an obvious inhibition capability on heat release.

Other combustion parameters of PLA and CNTs-H-C/PLA measured by cone calorimeter are also provided in Table 2. As can be seen in Table 2, the ignition time (TTI) of CNTs-H-C/PLA and PLA are close, while the pk-HRR/TTI that characterizes potential flashover[34] is reduced from 24.03 kW (m^2 s^{-1}) of PLA to 14.6 kW (m^2 s^{-1}) of CNTs-H-C/PLA-5, decreased by 39.2%. This indicates that the potential flashover of CNTs-H-C/PLA is significantly lower than that of PLA, which will greatly reduce the fire hazard. In addition, we note that the mass loss rate (av-

Table 2 Cone calorimeter test results[a]

Sample	PLA	CNTs-H-C/PLA-1	CNTs-H-C/PLA-3	CNTs-H-C/PLA-5
TTI (s)	23	23	23	24
pk-HRR (kW m^{-2})	552.6	420.9	392.1	350.8
Time to pk-HRR (s)	314	262	67	63
pk-HRR/TTI (kW (m^2 s^{-1}))	24	18	17	14
THR (MJ m^{-2})	157	123	140	151
av-MLR (g s^{-1})	0.16	0.10	0.08	0.06

[a] Note: TTI: ignition time, pk-HRR: peak value of heat release rate (HRR), THR: total heat release, av-MLR: average mass loss rate; pk-HRR/TTI indicates the potential flashover.

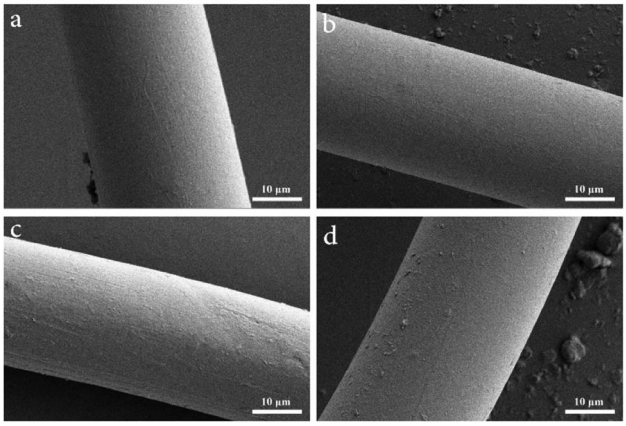

Fig. 4 SEM images of CNTs-H-C/PLA fibers with different content of CNTs-H-C 0.5 wt% (a), 1.0 wt% (b), 1.5 wt% (c), 2.0 wt% (d).

MLR) of CNTs-H-C/PLA is reduced compared with PLA, which means that CNTs-H-C has a condensed phase flame retardancy effect on PLA,[35] *i.e.*, a protective char layer is formed during the combustion process. On the one hand, the char layer can inhibit the outward diffusion of volatiles, and on the other hand, it can protect the internal matrix, thereby slowing down the mass loss rate and the heat release rate.

Cross-section morphology of CNTs-H-C/PLA composites

SEM images of the tensile section of pure PLA and CNTs-H-C/PLA composites were obtained to unveil the composite interface. The tensile section of pure PLA is relatively flat, showing a brittle section (Fig. 3c). With the introduction of CNTs-H-C, the roughness of the tensile section of the CNTs-H-C/PLA composite increased, and the cross-section cracks were clearly visible, and the CNTs-H-C was still embedded in the PLA matrix and was not pulled out during fracture, indicating the good interfacial bonding between CNTs-H-C and PLA matrix. In addition, no obvious agglomerates were seen in Fig. 3d and e, indicating that CNTs-H-C ($\leq$3 wt%) could be uniformly dispersed in PLA matrix. However, agglomerates appeared when the content of CNTs-H-C increased to 5 wt%, as shown in Fig. 3f.

Morphology, flame retardancy and mechanical properties of CNTs-H-C/PLA fibers

CNTs-H-C/PLA fibers were fabricated through melt spinning. And the morphology, flame retardancy and mechanical properties of CNTs-H-C/PLA fibers were thoroughly examined. SEM images of CNTs-H-C/PLA fibers with different flame retardant contents were acquired to observe the surface morphology. As shown in Fig. 4, the surface roughness of the CNTs-H-C/PLA fiber increases with the increase of the CNTs-H-C. When the CNTs-H-C content was over 1.0 wt%, agglomerates emerged on the fiber surface (white bright spots in Fig. 4c), and when the CNTs-H-C content reached 2.0 wt%, a few grooves and cracks can be observed on the fiber surface (Fig. 4d), which might have a negative impact on the flame retardancy and mechanical performances.

LOI test was conducted to reveal the flame retardant properties of the fibers. Table 3 shows that the LOI value of pure PLA fiber is only 20.0%, and the LOI of CNTs-H-C/PLA fiber first increases and then decreases with the increase of CNTs-H-C content. And the LOI value of CNTs-H-C/PLA fiber reaches 26.5% at the CNTs-H-C content of 1.0 wt%. This phenomenon is similar to the LOI results of CNTs-H-C/PLA composites. As confirmed in Fig. 4d, excessive flame retardant (over 2.0 wt%) is more likely to agglomerate in the fiber to form a heat concentration point, which would cause the fiber melt off.

The tensile strength and elongation at break of CNTs-H-C/PLA fibers were tested to investigate the mechanical property of the composite fibers. It can be seen from Table 3 that with the increase of the amount of CNTs-H-C, the breaking strength and elongation first increased and then decreased, and reached the maximum when the CNTs-H-C content was 1.0 wt%. The breaking strength and elongation of CNTs-H-C/PLA-1 fibers were 17 cN/dtex and 57%, respectively, which were 28.2% and 30.4% higher than those of pure PLA fibers, suggesting that CNTs-H-C are able to effectively strengthen and toughen PLA fibers.

Research on flame retardant mechanism

Further, the thermal decomposition behavior and char formation of pure PLA and CNTs-H-C/PLA-5 were analyzed to reveal the flame retardant mechanism. TG and DTG curves of PLA and CNTs-H-C/PLA were obtained to characterize the thermal decomposition behavior. As can be seen from Fig. 5a and b, PLA and CNTs-H-C/PLA present similar weight loss stage, while the maximum weight loss temperature increases from 355 °C for PLA to 360 °C for CNTs-H-C/PLA, which means that the introduction of CNTs-H-C could inhibit the thermal decomposition process of PLA. Moreover, the mass residue at 800 °C (MR 800 °C = 5.67%) of CNTs-H-C/PLA is higher than the theoretical MR 800 °C value (3.82%) of CNTs-H-C/PLA, calculated according to the TG results of CNTs-H-C. This suggests that CNTs-H-C

Table 3 LOI values and mechanical properties of CNTs-H-C/PLA fibers

		CNTs-H-C/PLA fibers with various flame retardant content (wt%)			
Properties	PLA fiber	0.5	1.0	1.5	2.0
LOI (%)	20.0	23.1	26.5	26.1	25.9
Tensile strength (cN/dtex)	13 ± 0.3	15 ± 0.4	17 ± 0.7	16 ± 0.7	15 ± 0.5
Breaking elongation (%)	44 ± 0.9	50 ± 1.3	57 ± 1.5	53 ± 0.9	46 ± 1.6

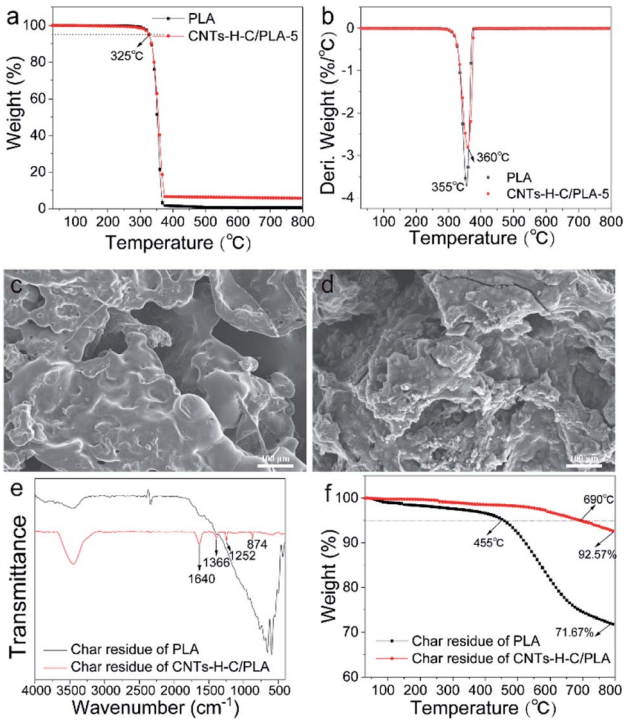

Fig. 5 TG (a) and DTG (b) curves of PLA and CNTs-H-C/PLA composites; SEM images (c and d), Infrared spectra (e) and TG curves (f) of the char residues of PLA and CNTs-H-C/PLA.

can promote the carbonization of PLA. The more carbon residues formed at high temperature, the less the thermal decomposition occurs during combustion,[36,37] which is one of the main reasons for the decrease in the heat release rate of CNTs-H-C/PLA.

Hereafter, the morphology, structure and thermal stability of the char residue of PLA and CNTs-H-C/PLA were studied to explore the flame retardant mechanism. SEM images of the char residue after combustion of PLA and CNTs-H-C/PLA are shown in Fig. 5c and d. The char layer of pure PLA is thin and smooth, and there are many bulging bubbles and small pores on the surface, which is due to the overflow of gaseous products generated by the combustion of PLA. In contrast, the char layer of CNTs-H-C/PLA is denser and has no pores. In addition, the surface of the char layer of CNTs-H-C/PLA is rough, and it is obvious that a large number of carbonaceous particles are deposited in the char layer. This indicates that the CNTs in the flame retardant gradually form the deposition skeleton of carbonaceous particles during the combustion, and the carbon skeleton carries and combines the pyrolysis products of the flame retardant system, thereby forming a dense and effective protective char layer. During combustion, the char layer can effectively block heat and oxygen, block the diffusion of volatile gases, and protect the internal matrix,[38] that is, CNTs-H-C has a notable condensed phase flame retardant effect on PLA.

The FTIR spectra of the char residue were provided in Fig. 5e. The char residue of PLA is mainly composed of compounds containing carbonyl (1725 cm^{-1}) and aliphatic hydrocarbons (400–800 cm^{-1}) generated by decarboxylation and main chain scission.[39] In contrast, the char residue of CNTs-H-C/PLA represents a broad peak around 3450 cm^{-1} formed by the overlapping of the hydrogen-bonded and –NH stretching vibration peaks derived from chitosan, and C=N stretching vibration peak at 1640 cm^{-1} attributed to the heterocyclic aromatic compounds, which could contribute to the formation of flame-retardant coke.[39] In addition, the P=N stretching vibration peak at 1366 cm^{-1}, and the P–N stretching vibration peaks at 1256 cm^{-1} and 874 cm^{-1} assigned to the HCCP of the CNTs-H-C can be observed in Fig. 5e. And the phosphorus-nitrogen skeleton of HCCP is very stable and can be partially retained even at high temperature,[40] which helps to improve the thermal stability of the char layer.

TG curves of PLA and CNTs-H-C/PLA char residues were determined, as shown in Fig. 5f. The thermal stability of the char residue of CNTs-H-C/PLA is significantly improved compared with that of pure PLA. The initial weight loss temperature of char residue increases from 455 °C for PLA to 690 °C for CNTs-H-C/PLA, increased by 235 °C. Besides, the residual mass (92.57%) of char residue of CNTs-H-C/PLA is much higher than that of pure PLA (71.67%), which means the introduction of CNTs-H-C produces more pyrolysis products with high temperature resistance, thereby improving the thermal stability of the char layer.

Conclusions

In conclusion, we have developed a CNT-based composite flame retardant with reinforced and toughened properties for PLA. The CNTs-H-C was prepared with CNTs as the core, hexachlorocyclotriphosphazene as the bridge, and chitosan grafted on the surface. CNTs-H-C/PLA composites and fibers were harvested by melt-blending and melt-spinning method. We show that the prepared CNTs-H-C displayed good compatibility and dispersion in PLA matrix; when blended with CNTs-H-C, CNTs-H-C/PLA composite exhibited outstanding flame retardancy with LOI increasing from 20.0% to 27.3%, UL94 rating reaching V-0. More importantly, the introduction of CNTs-H-C does not affect the spinnability of PLA, and LOI value of PLA fibers increased by 32.5% with addition of 1.0 wt% CNTs-H-C. Meanwhile, the breaking strength and elongation of CNTs-H-C/PLA fibers increased by 28.2% and 30.4%, compared with pure PLA fibers, verifying the strengthening and toughening properties of CNTs-H-C. Further, we revealed that CNTs-H-C/PLA exhibited a typical condensed phase flame-retardant mechanism. In short, a multifunctional CNT-based flame retardant was synthesized and applied in PLA matrix, displaying outstanding flame retardancy and simultaneously reinforced and toughened properties. Thus, the prepared CNTs-H-C showed great potential in polymer flame retardancy and mechanical enhancement.

Author contributions

Yunchao Xiao: methodology, investigation, data curation, writing – original draft preparation. Yaru Yang: conceptualization, visualization, supervision, resources, funding acquisition,

project administration, writing – review & editing. Qiulan Luo: formal analysis, resources. Bolin Tang: formal analysis, resources. Jipeng Guan: investigation, data curation. Qiang Tian: resources.

Conflicts of interest

There are no conflicts to declare.

Acknowledgements

This work was funded by the Natural Science Foundation of Zhejiang Province (LQ21E030008, LQ22C100002), and the Jiaxing Public Welfare Research Program (2022AY10014).

Notes and references

1 A. L. Coolen, C. Lacroix, P. Mercier-Gouy, E. Delaune and B. Verrier, Poly(lactic acid) nanoparticles and cell-penetrating peptide potentiate mRNA-based vaccine expression in dendritic cells triggering their activation, *Biomaterials*, 2018, **195**, 23–37.

2 Y. Xue, M. Shen, Y. Zheng, W. Tao, Y. Han, W. Li, P. Song and H. Wang, One-pot scalable fabrication of an oligomeric phosphoramide towards high-performance flame retardant polylactic acid with a submicron-grained structure, *Composites, Part B*, 2019, **183**, 107695.

3 Y. Xue, J. Feng, Z. Ma, L. Liu, Y. Zhang, J. Dai, Z. Xu, S. Bourbigot, H. Wang and P. Song, Advances and challenges in eco-benign fire-retardant polylactide, *Mater. Today Phys.*, 2021, **21**, 100568.

4 A. Z. Naser, I. Deiab and B. M. Darras, Poly(lactic acid) (PLA) and polyhydroxyalkanoates (PHAs), green alternatives to petroleum-based plastics: a review, *RSC Adv.*, 2021, **11**, 17151–17196.

5 J. Feng, X. Xu, Z. Xu, H. Xie, P. Song, L. Li, G. Huang and H. Wang, One-pot, solvent- and catalyst-free synthesis of polyphosphoramide as an eco-benign and effective flame retardant for poly(lactic acid), *ACS Sustainable Chem. Eng.*, 2020, **8**, 16612–16623.

6 Y. Zhang, J. Jing, T. Liu, L. Xi, T. Sai, S. Ran, Z. Fang, S. Huo and P. Song, A molecularly engineered bioderived polyphosphate for enhanced flame retardant, UV-blocking and mechanical properties of poly(lactic acid), *Chem. Eng. J.*, 2021, **411**, 128493.

7 H. Yang, B. Shi, Y. Xue, Z. Ma, L. Liu, L. Liu, Y. Yu, Z. Zhang, P. K. Annamalai and P. Song, Molecularly engineered lignin-derived additives enable fire-retardant, UV-shielding, and mechanically strong polylactide biocomposites, *Biomacromolecules*, 2021, **22**, 1432–1444.

8 T. Bai, B. Zhu, H. Liu, Y. Wang, G. Song, C. Liu and C. Shen, Biodegradable poly(lactic acid) nanocomposites reinforced and toughened by carbon nanotubes/clay hybrids – ScienceDirect, *Int. J. Biol. Macromol.*, 2020, **151**, 628–634.

9 Y. Zhang, J. Jing, T. Liu, L. Xi and P. Song, A molecularly engineered bioderived polyphosphate for enhanced flame retardant, UV-blocking and mechanical properties of poly(lactic acid), *Chem. Eng. J.*, 2021, **411**, 128493.

10 J. Feng, Z. Ma, Z. Xu, H. Xie, Y. Lu, C. Maluk, P. Song, S. Bourbigot and H. Wang, A Si-containing polyphosphoramide via green chemistry for fire-retardant polylactide with well-preserved mechanical and transparent properties, *Chem. Eng. J.*, 2021, **431**, 134259.

11 Y. Yu, L. Xi, M. Yao, L. Liu, Y. Zhang, S. Huo, Z. Fang and P. Song, Governing effects of melt viscosity on fire performances of polylactide and its fire-retardant systems, *iScience*, 2022, **25**, 103950.

12 X. Xu, J. Dai, Z. Ma, L. Liu, X. Zhang, H. Liu, L. Tang, G. Huang, H. Wang and P. Song, Manipulating interphase reactions for mechanically robust, flame-retardant and sustainable polylactide biocomposites, *Composites, Part B*, 2020, **190**, 107930.

13 Y. Chen, W. Wang, Y. Qiu, L. Li, L. Qian and F. Xin, Terminal group effects of phosphazene-triazine bi-group flame retardant additives in flame retardant polylactic acid composites, *Polym. Degrad. Stab.*, 2017, **140**, 166–175.

14 Y. Guo, M. Xiao, Y. Ren, Y. Liu, Y. Wang, X. Guo and X. Liu, Synthesis of an effective halogen-free flame retardant rich in phosphorus and nitrogen for lyocell fabric, *Cellulose*, 2021, **28**, 7355–7372.

15 X. Wang, W. He, L. Long, S. Huang and G. Xu, A phosphorus- and nitrogen-containing DOPO derivative as flame retardant for polylactic acid (PLA), *J. Therm. Anal. Calorim.*, 2020, **145**, 331–343.

16 S. Qiu, J. Sun, H. Li, X. Gu, B. Fei and S. Zhang, A green way to simultaneously enhance the mechanical, flame retardant and anti-ultraviolet aging properties of polylactide composites by the incorporation of tannic acid derivatives, *Polym. Degrad. Stab.*, 2022, **196**, 109831.

17 C. Chazot, C. K. Jons and A. J. Hart, In Situ Interfacial Polymerization: A Technique for Rapid Formation of Highly Loaded Carbon Nanotube-Polymer Composites, *Adv. Funct. Mater.*, 2020, **2005499**, 1–12.

18 J. Liu, C. Chen, Y. Feng, Y. Liao, Y. S. Ye, X. Xie and Y. W. Mai, Ultralow-Carbon Nanotube-Toughened Epoxy: The Critical Role of a Double-Layer Interface, *ACS Appl. Mater. Interfaces*, 2017, **10**, 1204–1216.

19 T. Kashiwagi, F. Du, J. F. Douglas, K. I. Winey, R. Harris and J. R. Shields, Nanoparticle networks reduce the flammability of polymer nanocomposites, *Nat. Mater.*, 2005, **4**, 928.

20 T. Sai, S. Ran, Z. Guo, P. Song and Z. Fang, Recent advances in fire-retardant carbon-based polymeric nanocomposites through fighting free radicals, *SusMat*, 2022, DOI: **10.1002/sus2.73**.

21 P. V. Polydoropoulou, C. V. Katsiropoulos and S. G. Pantelakis, The synergistic effect of CNTs and flame retardants on the mechanical behavior of aerospace epoxy resin, *Polym. Eng. Sci.*, 2017, **57**, 528–536.

22 S. Zhang, Y. Jiang, Y. Sun, J. Sun and X. Gu, Preparation of flame retardant and conductive epoxy resin composites by incorporating functionalized multialled carbon nanotubes and graphite sheets, *Polym. Adv. Technol.*, 2021, **32**, 2093–2101.

23 B. Xue, Y. Song, Y. Peng, J. Bai and Y. Yang, Enhancing the flame retardant of polyethylene terephthalate (PET) fiber via incorporation of multi-walled carbon nanotubes based phosphorylated chitosan, *J. Text. Inst.*, 2018, **109**, 871–878.

24 X. Liu, X. Gu, J. Sun and S. Zhang, Preparation and characterization of chitosan derivatives and their application as flame retardants in thermoplastic polyurethane, *Carbohydr. Polym.*, 2017, **167**, 356.

25 R. Chen, Z. Luo, X. J. Yu, H. Tang and H. Zhou, Synthesis of chitosan-based flame retardant and its fire resistance in epoxy resin, *Carbohydr. Polym.*, 2020, **245**, 116530.

26 Q. Shi, C. Ren and B. Cheng, Flame retardant treatment of jute fabric with chitosan and sodium alginate, *Polym. Degrad. Stab.*, 2022, **196**, 109826.

27 W. Meng, H. Wu, X. Bi, Z. Huo, J. Wu, Y. Jiao, J. Xu, M. Wang and H. Qu, Synthesis of ZIF-8 with encapsulated hexachlorocyclotriphosphazene and its quenching mechanism for flame-retardant epoxy resin, *Microporous Mesoporous Mater.*, 2021, **314**, 110885.

28 K. Rhili, S. Chergui, A. S. Eldouhaibi and M. Siaj, Hexachlorocyclotriphosphazene Functionalized Graphene Oxide as a Highly Efficient Flame Retardant, *ACS Omega*, 2021, **6**, 6252–6260.

29 M. Hou, A. Li, W. Zou, H. Li and C. Zhang, Effect of Amino-Modified Carbon Nanotubes on the Pore Structure of Polyurethane Foams, *Polym. Mater. Sci. Eng.*, 2016, **32**, 179–183.

30 D. J. Ando, *Infrared Spectroscopy: Fundamentals and Applications*, John Wiley & Sons, Ltd, 2005.

31 Y. Shi and L. J. Li, Chemically modified graphene: flame retardant or fuel for combustion?, *J. Mater. Chem.*, 2011, **21**, 3227–3279.

32 V. Babrauskas, The Cone Calorimeter, *SFPE Handbook of Fire Protection Engineering*, 2016.

33 L. Costes, F. Laoutid, M. Aguedo, A. Richel, S. Brohez, C. Delvosalle and P. Dubois, Phosphorus and nitrogen derivatization as efficient route for improvement of lignin flame retardant action in PLA, *Eur. Polym. J.*, 2016, **84**, 652–667.

34 A. Olad, F. Maryami, A. Mirmohseni and A. A. Shayegani-Akmal, Potential of slippery liquid infused porous surface coatings as flashover inhibitors on porcelain insulators in icing, contaminated, and harsh environments, *Prog. Org. Coat.*, 2021, **151**, 106082.

35 Y. Xia, G. Q. Zhu, Y. J. Gao and F. Guo, Use of Cone Calorimeter for Estimating Fire Behavior of PVC Membranes, *Procedia Eng.*, 2018, **211**, 810–817.

36 P. Jia, M. Zhang, C. Liu, L. Hu, G. Feng, C. Bo and Y. Zhou, Effect of chlorinated phosphate ester based on castor oil on thermal degradation of poly(vinyl chloride) blends and its flame retardant mechanism as secondary plasticizer, *RSC Adv.*, 2015, **5**, 41169–41178.

37 G. Huang, W. Chen, T. Wu, H. Guo, C. Fu, Y. Xue, K. Wang and P. Song, Multifunctional graphene-based nano-additives toward high-performance polymer nanocomposites with enhanced mechanical, thermal, flame retardancy and smoke suppressive properties, *Chem. Eng. J.*, 2020, **410**, 127590.

38 Q. Yong, L. Qian and X. Wang, Flame-retardant effect of a novel phosphaphenanthrene/triazine-trione bi-group compound on an epoxy thermoset and its pyrolysis behaviour, *RSC Adv.*, 2016, **6**, 56018–56027.

39 H. Zou, C. Yi, L. Wang, H. Liu and W. Xu, Thermal degradation of poly(lactic acid) measured by thermogravimetry coupled to Fourier transform infrared spectroscopy, *J. Therm. Anal. Calorim.*, 2009, **97**, 929–935.

40 J. Dong, Z. Mao and Z. Chen, Toughening, highly thermostable, and flame retardant polylactic acid enabled by polyphosphazene microsphere, *J. Appl. Polym. Sci.*, 2022, **139**, 51973.